We are IntechOpen,
the world's leading publisher of
Open Access books
Built by scientists, for scientists

6,900
Open access books available

186,000
International authors and editors

200M
Downloads

154
Countries delivered to

Our authors are among the

TOP 1%
most cited scientists

12.2%
Contributors from top 500 universities

CLARIVATE ANALYTICS
BOOK CITATION INDEX
INDEXED

WEB OF SCIENCE™

Selection of our books indexed in the Book Citation Index
in Web of Science™ Core Collection (BKCI)

Interested in publishing with us?
Contact book.department@intechopen.com

Numbers displayed above are based on latest data collected.
For more information visit www.intechopen.com

Spin Labels in the Gel Phase and Frozen Lipid Bilayers: Do They Truly Manifest a Polarity Gradient?

Boris Dzikovski and Jack Freed

Additional information is available at the end of the chapter

1. Introduction

Lipid spin labels containing nitroxide groups at different positions in the fatty acid chain, such as 1-palmitoyl-2-stearoyl-(n-doxyl)-sn-glycero-3-phosphocholines (n-PC spin labels) are a useful and proven tool in lipid research. They have provided important insights into the structure of model and biological membranes, reported on the membrane fluidity, polarity, phase state and presence of microscopic domains[1], accessibility of different depth positions in the lipid bilayer for oxygen and other polar and non-polar paramagnetic compounds[2-4] and protein/lipid interactions [5, 6].

It is generally accepted, that, unlike bulky fluorescent labels[7,8], nitroxides are well incorporated into fluid lipid bilayers[9] and not excluded from them. However, it has been shown by NMR that although the most probable location of the nitroxide group for 5-, 10- and 16- PC spin labels in the fluid POPC membrane corresponds to the fully extended conformation, the distribution is relatively broad and other conformations should also be present[10]. Bent conformations were previously found for doxylstearic acids in monomolecular films[11], water/hydrocarbon emulsion particles[12] and micellar systems[13]. In fluid membranes the fluidity, polarity and accessibility parameters reported by ESR using PC spin labels and n-doxylstearic acids are, in general, change monotonically with an increase in n[3, 14], although there are indications that the spin label groups on the stearates are located nearer to the membrane exterior than the analogous positions of the unlabeled phospholipid chains[15]. However, in the gel phase, which is characterized by denser chain packing and higher order, the preferential location may be different.

In this chapter we focus on the behavior of PC spin labels in the gel phase and frozen membranes. We show how the superior g-factor resolution of HF ESR provides new insights

INTECH
open science | open minds

in this behavior and a new look at the vast body of experimental data accumulated with PC spin labels in the last 30 years. In particular, we revisit so-called "polarity profiles" determined from the g-factor values and hyperfine splittings of PC spin labels in frozen phospholipid membranes with or without cholesterol and show that these values are affected by a number of factors in the membrane composition, chain packing in the lipid phase and folding properties of the *sn-2* spin labeled chain PC labels rather than reflect gradients of polarity or water content present in the membrane[16].

2. Resolution of different hydrogen-bond states by 240GHz ESR in bulk organic solvents

It has been well established that the g-tensor and hyperfine components of nitroxide radicals are very sensitive to the local environment, to polarity and proticity in particular. In general, changing the local environment of the nitroxide moiety from water (polar) to hydrocarbon (non-polar) causes an increase in the g-tensor components and a concomitant decrease in the values of the components of the hyperfine tensor. This effect is most pronounced for the tensor components g_{xx} and A_{zz}. However, the separation of the polarity and proticity effects could complicate the analysis of the ESR spectra. Proticity refers to the propensity to donate hydrogen bonds; whereas aprotic refers to solvents which cannot donate a hydrogen bond. At relatively low frequencies, up to 95GHz, the separation of hydrogen-bonded vs. non hydrogen-bonded states of the nitroxide often relied upon different g versus A plots, discovered for these two states[17]. However, as shown in a recent study using TEMPO, if the correlations are indeed different for TEMPO in protic and aprotic solvents, the difference is rather small[18].

On the other hand, superior g-factor resolution of HF ESR allows for observation of two resolved spectral components corresponding to two (Smirnova et al.[19] at 130GHz) or possibly more (Bordignon et al.[20] at 95, 275 and 360GHz) states of hydrogen-bonding. Two hydrogen bonding states coexisting in frozen deuterated alcohols were previously demonstrated for perdeuterated TEMPONE by X-band ESR[21].

Tables 1 and 2 show the values of A_{zz} and a_{iso} hyperfine splitting and the g_{xx} component of the g-tensor for several nitroxide radicals.

As one sees from Fig.1, whereas at X-band one sees a continuous increase in the ^{14}N hyperfine splitting with change of the local environment from non-polar/aprotic to polar/protic, the 240 GHz ESR shows three distinct values of the g_{xx} parameter. Although the presence/ratio of these components strongly depends on the polarity-proticity of the solvent, there is little variation in the g_{xx} measured for each such component. For all four spin labels studied three distinct components could be detected: (1) "non-polar", as in toluene, DBPh or the minor component in alcohols, (2) "polar", the major component for ethanol and major or minor component in TFE and water/glycerol , depending on the nitroxide used, and (3) "very polar" component observable in TFE and water/glycerol. Although components 2 and 3 cannot be separated at 240GHz as two distinct peaks, their presence is quite obvious (compare Figs.1A-D for different nitroxides). We assign these components to different

Solvent, dielectric constant at room temperature[51]	Oxo-TEMPO	TEMPO	4-Hydroxy TEMPO	3-carboxy-2,2,5,5 tetramethylpyrrolidine - 1-oxyl
Isopentane, 1.8	14.27/**	15.29/68.2	15.15/**	13.92/**
MCH, 2.02	14.315/**	15.32/68.2	15.20/**	13.96/**
Toluene, 2.4	14.49/67.6	15.53/69.3	15.43/69.1	14.22/66.7
DBPh, 6.4	14.61/67.6	15.64/69.4	15.55/69.2	14.37/66.9
Ethanol, 24.3	15.06/70.0	16.21/72.9	16.05/71.0	15.02/70.1
TFE, 26.14	15.63/73.5	17.00/79.7	16.73/77.3	15.77/74.4
Water/Glycerol, 80.4	15.97/73.8	17.19/76.5	16.96/75.5	16.12/73.2

** $2A_{zz}$ value at 77K cannot be reliably determined due to the presence of a singlet-like background.

Table 1. Values of isotropic hyperfine splitting constant a_{iso} and $2A_{zz}$ determined at X-band at 295 and 77K respectively for several solvents. These A_{zz} values were also used to obtain the best fits for the corresponding 240 GHz rigid limit spectra.

| Solvent, dielectric constant	Oxo-TEMPO	TEMPO	4-Hydroxy TEMPO	3-carboxy-2,2,5,5 tetramethylpyrrolidine - 1-oxyl
Toluene	2.009438	****	*****	****
DBPH	2.009445	2.010103	2.010129	2.009230
Ethanol	2.009485/**2.008838**	sh/2.009411	2.010040/**2.009456**	2.009250/**2.008533**
TFE	**2.008793**/sh	2.008669	2.009460/**2.009089**	2.008487/sh
Water/Glycerol	**2.008784**/~2.00850	2.008805	2.009460/**2.008951**	2.008532/sh

Table 2. g_{xx} component of the g-tensor determined by 240GHz ESR at 80-85K in several glass forming solvents. A common value of 2.00233 was assigned as g_{zz} for all spin labels and g_{xx} value was accurately determined relative to this g_{zz} value from the corresponding spectral splitting[29, 52]. If two components are present in the spectrum, the component with higher fraction is marked bold. "Sh" denotes the presence of a high/low field component, which manifests itself not as a distinct peak but as a shoulder on the main component.

hydrogen-bonding states of nitroxide radicals and speculate that state 2 corresponds to a single hydrogen bond, while state 3 is double-bonded. Existence of multiple hydrogen bonding to a nitroxide has been predicted theoretically[22-24] and later suggested as an explanation for complex ESR lineshapes observed in spin labeled proteins[20]. Interestingly, the g_{xx} value of the non-hydrogen bonded component for all four spin labels studied shows little dependence on the polarity of the frozen glass-forming solvent (Table 3). This contrasts with some theoretical predictions for the g-factor[25], as well as some room temperature measurements for g_{iso} pointing to a higher g-factor for lower dielectric constants ε[17, 18].

Tempone in different solvents, rigid limit

(A)
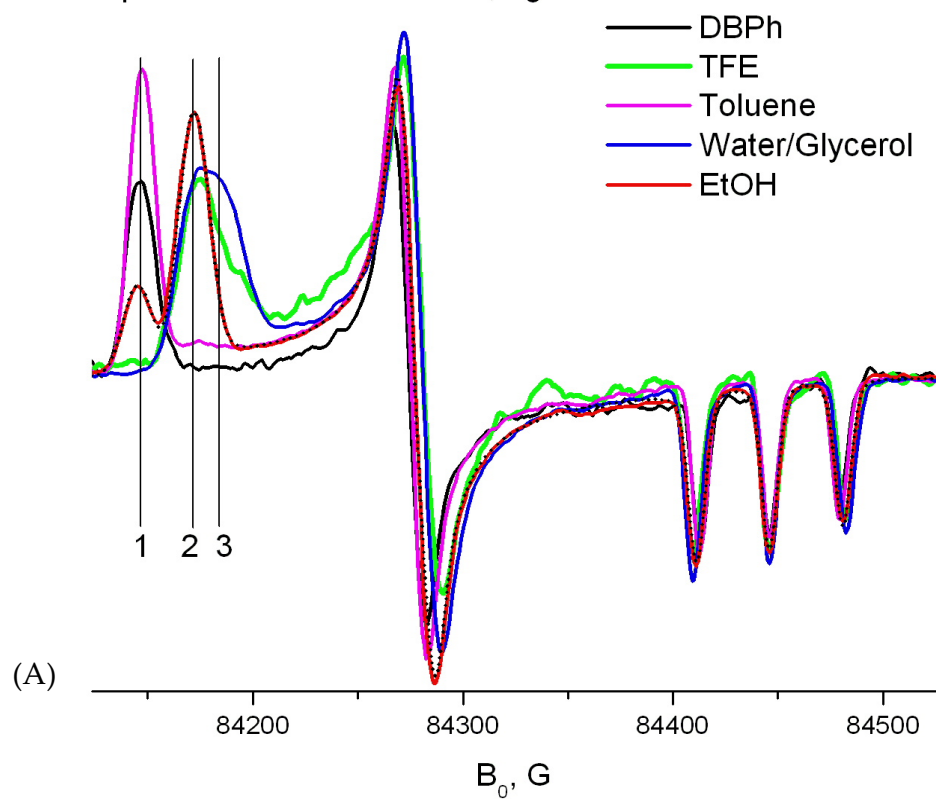
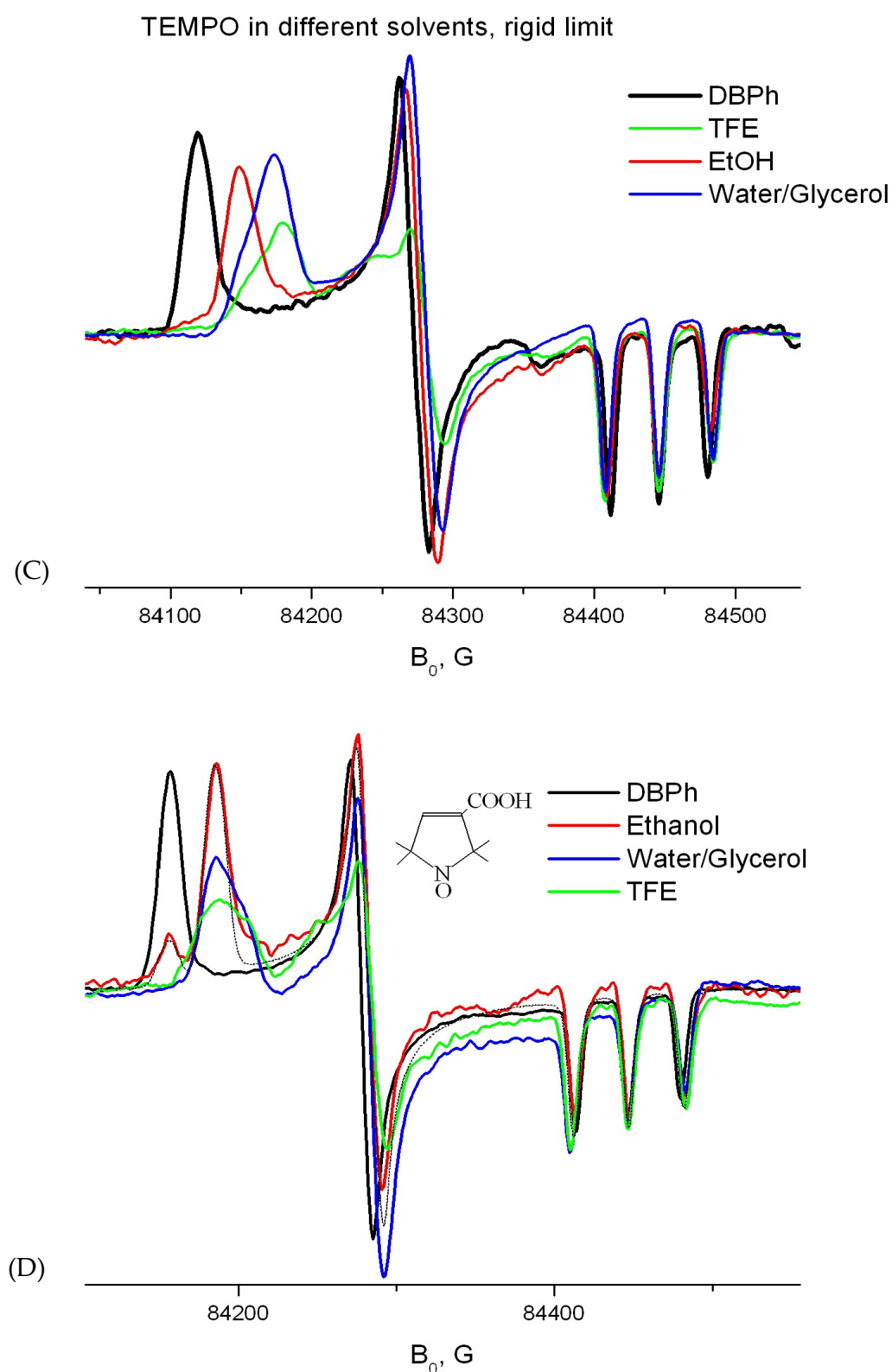Tempol in different solvents, rigid limit

(B)
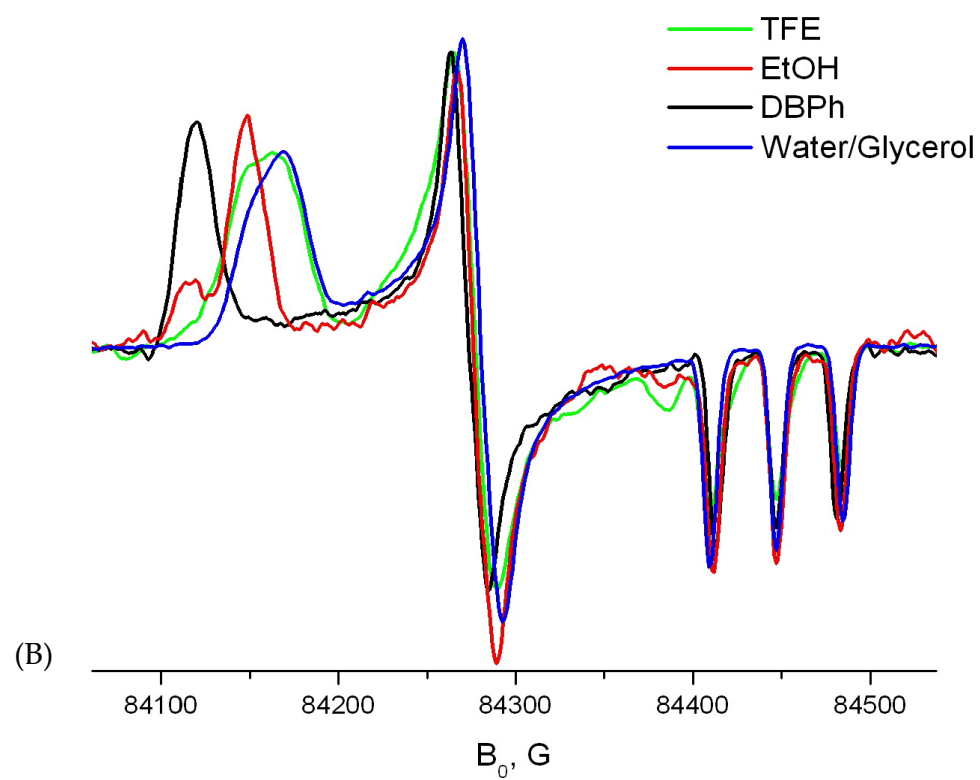
Figure 1. 240 GHz ESR spectra of 4-oxo-TEMPO (TEMPONE) (from [16]) (A), 4-hydroxy-TEMPO (TEMPOL) (B), TEMPO (C) and 2,2,5,5-Tetramethyl-3-pyrrolin-1-oxyl-3-carboxylic acid free radical (D) in a series of glass-forming solvents at 80-85K. Black dotted lines in A and D show two-component rigid simulation of the ethanol spectra. In (A), g values 2.009450, 2.008830 and 2.008500 are noted "1", "2" and "3" respectively.

	DMPC	DMPC/Chol	DPPC	DPPC/Chol
5	68.9	69.7	69.2	70.1
7	69.3	70.1	69.9 (broadening)	69.1
10	69.6	66.6	69.5 (more broadening)	66.5
12	68.4	66.3	67.2	66.4
14	69.3	66.4	66.3	66.8
16	69.3	66.2	66.7	66.5

Table 3. Hyperfine splitting parameter $2A_{zz}$ in DMPC and DPPC membranes with and without cholesterol determined by X-band ESR at 77K. To record the ESR spectra the samples in 1.2 mm ID capillaries after long exposure at 19^0C were quickly submerged into liquid nitrogen.

3. Membrane environment

3.1. X-band ESR

The full extent of the 9 GHz spectrum is determined by the largest of the principal values of the ^{14}N hyperfine constant, which is A_{zz}. Hence at X-band, the distance between outer extrema for a well-resolved spectrum in the rigid limit is exactly $2A_{zz}$. This value is known to increase ~ 2G if nitroxide is transferred from a non-polar solvent like hydrocarbons to water and, as mentioned above, can be considered a measure for local polarity. Table.3 shows the $2A_{zz}$ determined by X-band ESR as the outer splitting of the rigid limit spectra at 77K. As seen from the data, DMPC/Cholesterol (Fig. 2B) and DPPC/Cholesterol (Fig. 2D) membranes, consistent with previous observations[3], show abrupt drop in the $2A_{zz}$ value, between n-PC positions 7 and 10. However, for DMPC, in the absence of cholesterol, the $2A_{zz}$ value shows little trend throughout the PC spin labels series and remains ~ 69.5G (cf. Fig. 2A), which correspond to a relatively polar environment, more polar than ethanol (see below). DPPC in the absence of cholesterol (Fig. 2C), in general, shows a profile similar to a cholesterol-containing membrane, though the spectra, especially for positions 7-12 show signs of a broad singlet-like component.

The dependencies of relaxation enhancement $\Delta(1/P)$ by 10 mM of Ni(ClO$_4$)$_2$ on the spin-labeling position for the gel and liquid crystal phase of DMPC are given in Fig. 3. Here P is the relaxation parameter $P=g_e T_1 T_2$, where g_e is the electron gyromagnetic ratio and T_1 and T_2 are corresponding effective relaxation times. In the liquid crystal phase (T=39^{0}C) the interaction with the paramagnetic relaxant decreases with increasing n, consistent with an increase in the average immersion depth of the spin label moiety in the membrane. On the contrary, the $\Delta(1/P)$ profile in the gel phase (P$_\beta$, T=19^{0}C) is almost flat, with a minor spike at position 10.

3.2. High field/ High frequency ESR

High frequency ESR and PC spin labels were previously used to study polarity profiles in phospholipid membranes[14, 26, 27]. For example, in a detailed ESR study at 250GHz 5,7,10,12,14 and 16 PC were studied in DPPC and DPPC/gramicidin systems[26]. It was found that in pure DPPC most spins are strongly aggregated and the spectrum consists mostly (especially for
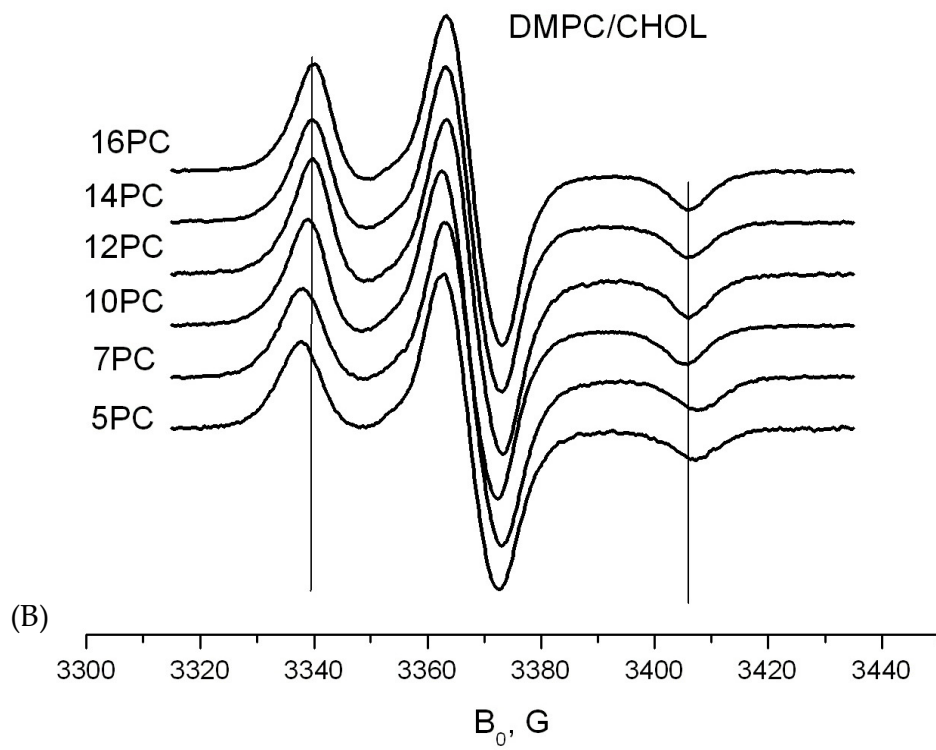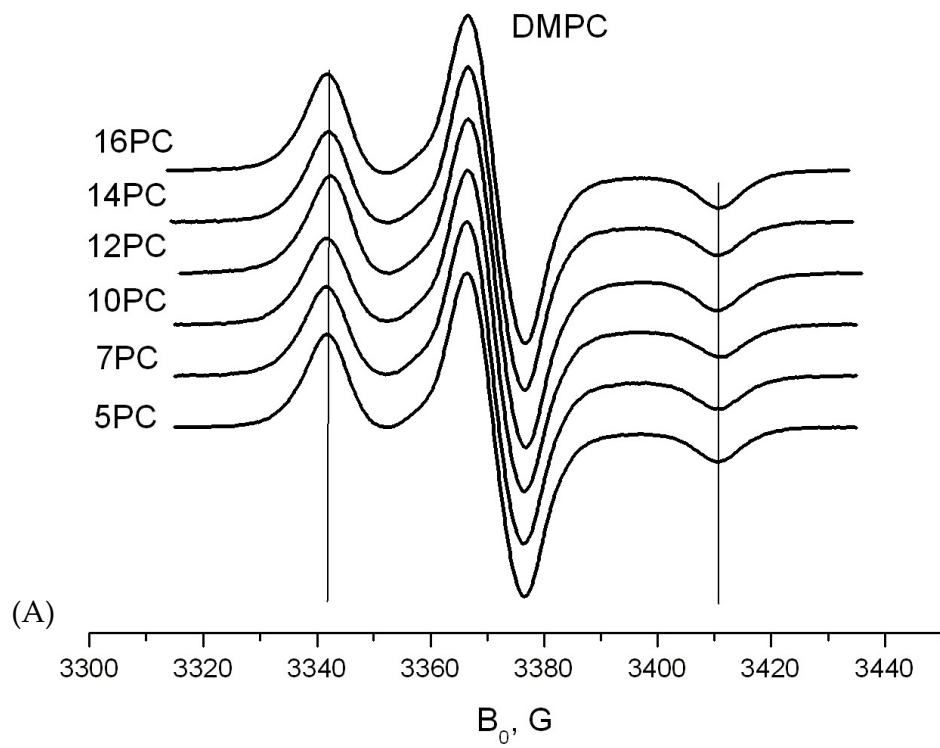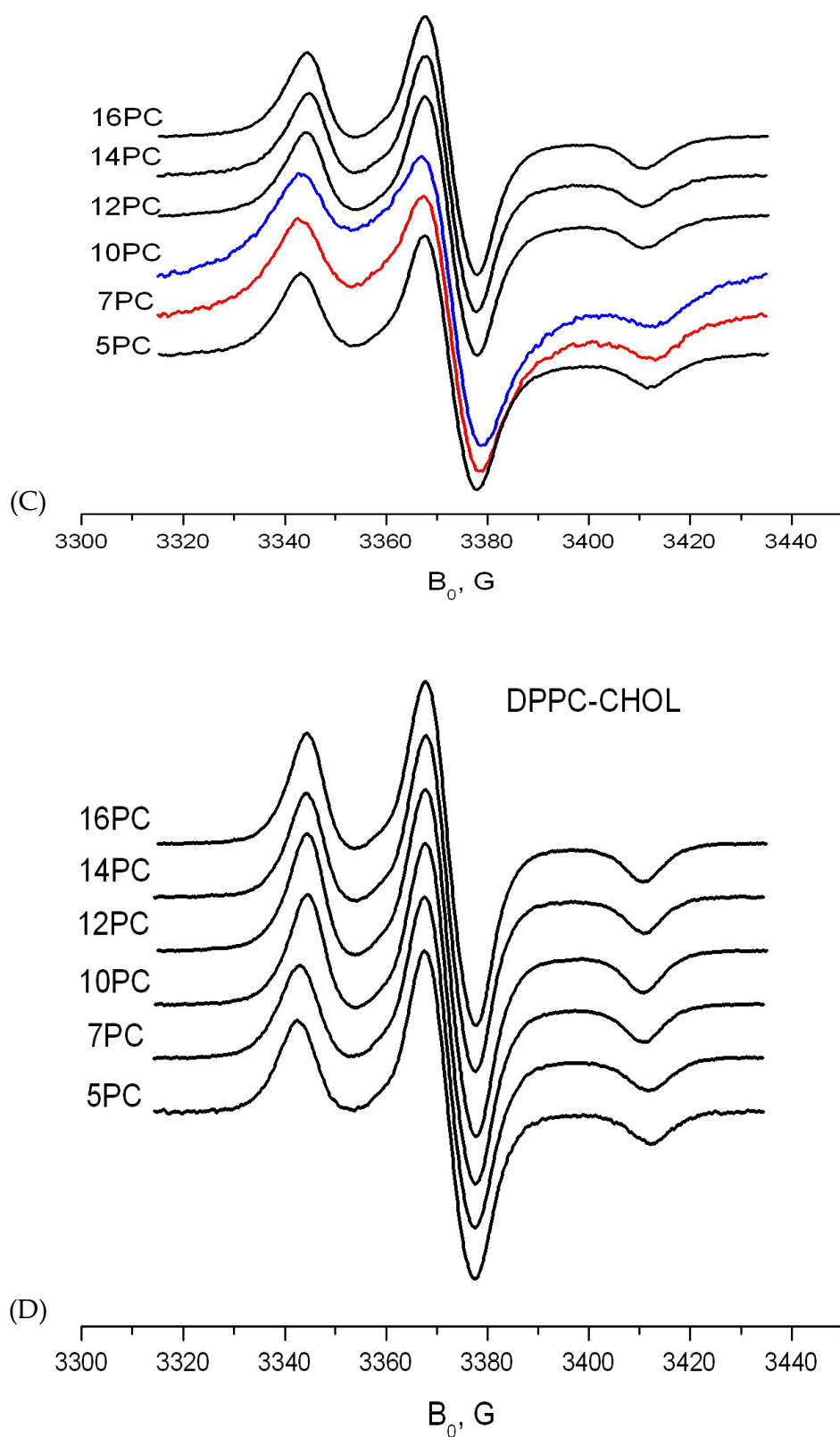
Figure 2. 9 GHz ESR spectra of PC spin labels in DMPC (A) (from [16]), DMPC/30% Cholesterol (B), DPPC (C) and DPPC/30% Cholesterol (D) at 77K. In (C) spectra of 7PC and 10 PC with most broadening are shown in color.
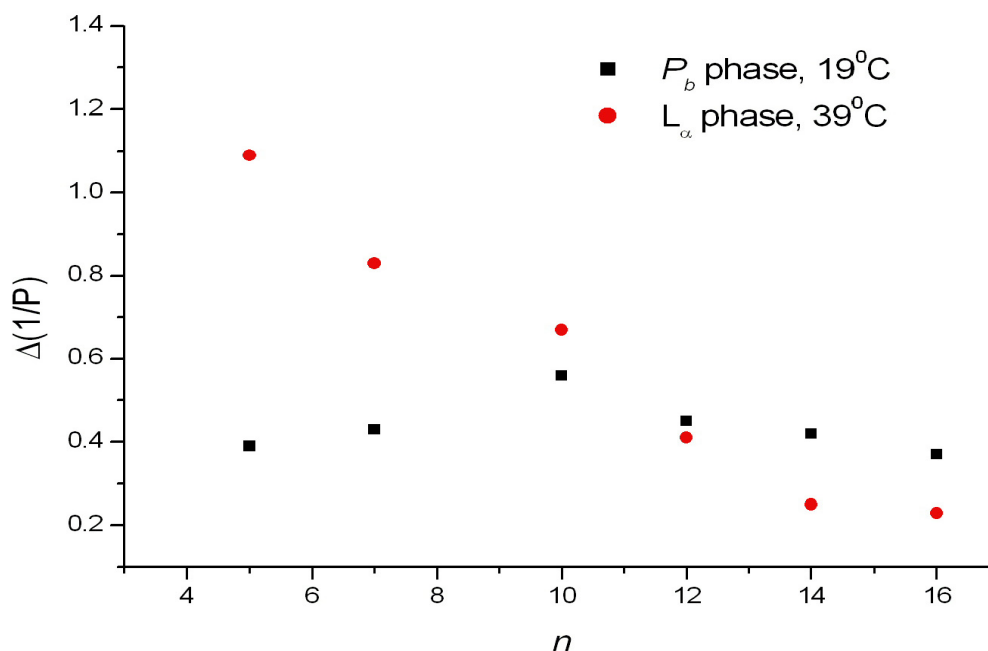
Figure 3. Relaxation enhancement from 10 mM of $Ni(ClO_4)_2$ introduced into the water phase of lipid DMPC dispersions as a function of n in the P_β (190C) and L_α (390C) lipid phases. An almost flat accessibility profile in the gel might indicate similar average membrane immersion depth for the nitroxide moieties of all studied PC labels (from [16]).

7-12 PCs) of a singlet-like signal. Although the g-factor values for the resolved rigid-limit component seems to indicate increasing immersion of the nitroxide into the hydrophobic core of the membrane with increasing n, it is difficult to obtain any information on the location of aggregates which manifest themselves in the broad component. However, addition of cholesterol prevents such aggregation and yields in better resolved spectra[27].

3.2.1. Frozen DMPC/DPPC membranes with cholesterol: Partition-like depth distribution of spin labels

Several W-band (94GHz) studies by Marsh and coworkers[14, 27, 28] on DMPC/Cholesterol membranes utilized all n-PC spin labels in the 4-16 range (except 15-PC). Based on the g_{xx} values detailed polarity profiles for these systems were suggested. These polarity profiles appeared to be similar to the polarity profiles previously obtained by rigid limit X-band ESR from the hyperfine splitting[3] values. However, a close inspection of the spectra of [27] shows two partially resolved components, which likely correspond to hydrogen-bonded and non-hydrogen-bonded states of the nitroxide radical. These two components are discernible not only for the area of abrupt "polarity change" (PC 5-10), but also for PC14-16. Higher resolution of 240GHz ESR allows for complete separation and identifying these components. Fig.4 A, B show the spectra for DMPC and DPPC in the presence of cholesterol. The ESR spectra in the two different lipids are very similar, nearly identical. There are two components discernible for n≥7, which are completely resolved for n≥10, with g_{xx}= 2.009435 and g_{xx}= 2.008820 (with g_{zz} taken as 2.00233, see [29]). The two g values are nearly the same for all n. For 5-PC only the polar component is present.
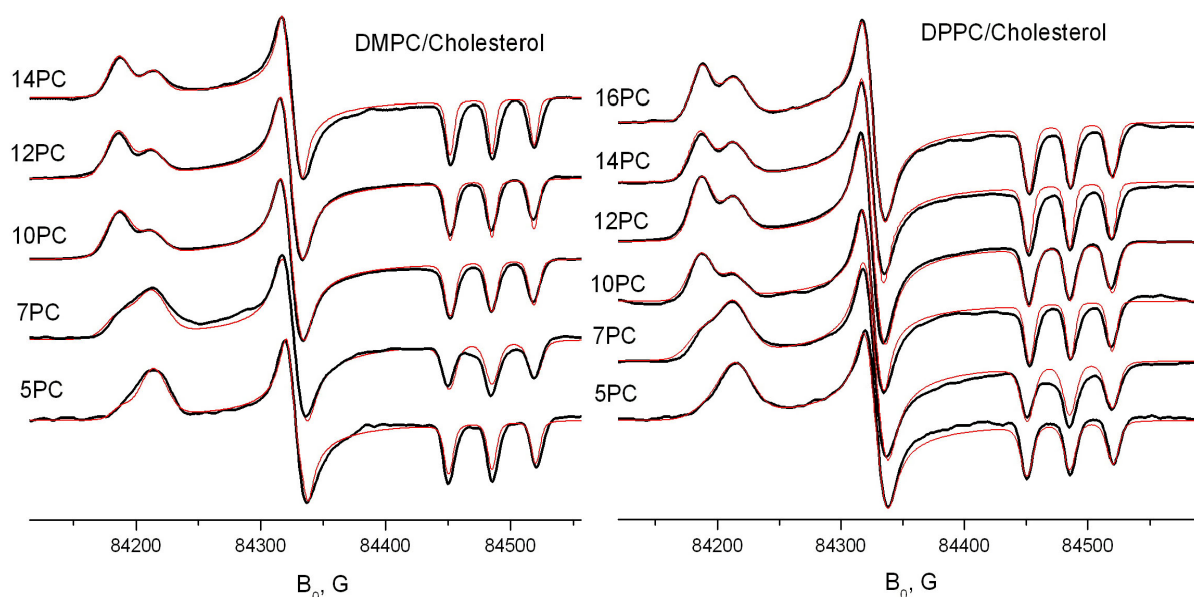
Figure 4. Rigid-limit 240 GHz ESR spectra of *n*-PC spin labels in DMPC and in DPPC containing 30% mol cholesterol. T=80-82K. The samples are gradually frozen in the flow of gaseous nitrogen. Red lines show simulations of these spectra using two components with the g_{xx} = 2.009435±0.000005 and 2.008820±0.000005 for all spectra. g_{yy} and g_{zz} are taken 2.006100 and 2.00233 for both components (from [16]).

Can these two components just reflect a water penetration profile? It has previously been assumed that polarity profile reported by spin labels for fluid and frozen membranes containing cholesterol in general follows the membrane water penetration profile[23, 30, 31]. However, the exact features of the ESR spectrum at low temperature may be defined by interplay of this water penetration and the flexibility of spin-labeled lipid chains, see below. While, due to the short acyl tether, the nitroxide of 5PC is always located in the area with higher water content and shows only hydrogen-bonded component, longer acyl tethers can reach a less polar area with lower water content. Yet, even for 14 and16PC there is a substantial fraction of hydrogen-bonded component. Moreover, the fraction of the hydrogen-bonded component does not decrease monotonically with an increase in the *n* number. As seen in Fig.4 A, B and Table 4, this fraction experiences a dramatic drop between 7 and 10PC and then gradually increases further for positions 12,14 and 16. Based on these observations and what is currently known about flexibility of spin-labeled lipids[10], we believe that the hydrogen-bonded component mainly corresponds to bent conformations of the spin-labeled lipid chain, rather than penetration of water molecules to the middle of the membrane and forming a hydrogen bond with the nitroxide moiety of the PC spin label in a fully extended conformation.

Indeed, theoretical estimates[32] show that the concentration of water in the middle of the DPPC membrane is ~ 1 mM. It should be even lower for membranes containing cholesterol, since cholesterol is known to substantially decrease water permeability across lipid membranes[33, 34]. For the equilibrium constant between hydrogen bonded/unbonded forms of 16-sasl in toluene - trifluoroethanol mixtures Marsh[30] gives a value ~ 1M^{-1}. This value is determined from the isotropic hyperfine splitting at room temperature. Our estimates for this constant for various nitroxides based on measurements of 2A$_{zz}$ values in ethanol –

PC label	Ratio HB/non-HB in DMPC	Ratio HB/non-HB in DPPC
5	~6	> 8
7	1.8	2.3
10	0.32	0.36
12	0.45	0.62
14	0.55	0.8
16	---	0.8

Table 4. Ratio of hydrogen bonded, HB (g_{xx}= 2.00882) and non-hydrogen bonded components (g_{xx}=2.009435) determined from rigid-limit simulations of n-PC spin labels in DMPC and DPPC containing 30% mol cholesterol.

DBPH mixtures by 9GHz ESR at 77K or on the ratio of hydrogen-bonded and non-hydrogen bonded components in frozen ethanol (~ 17M hydroxyl concentration) measured by 240GHz ESR give values of the same order, between $0.2M^{-1}$ and $0.5M^{-1}$. A 1:1 ratio of the two spectral components for a nitroxide located in the middle of the bilayer would thus yield a water concentration in the membrane core of ~0.5M, about three orders of magnitude higher than expected from theoretical estimates. Also, consistent with the above estimates of the equilibrium constant, in our test experiments we did not see any appearance of a hydrogen bonded component for nitroxides dissolved in frozen nearly saturated (~16 mM) solutions of water in toluene.

And finally, a strong point in favor of considering bent conformations of *n*-PC spin labels is the non-monotonic dependence of the hydrogen-bonded fraction on *n* (Table 4). In a fluid membrane the membrane depth distribution of nitroxide moieties for each spin-labeled lipid correlates to its *n*-value[10]. Higher *n* show deeper average immersion although the distribution is broad and even high *n* numbers show a substantial fraction of conformations with the nitroxide touching the carbonyl area. In the much denser packed gel phase the situation can be different and the spin labels may prefer defects in the lipid structure[35, 36]. One of the areas with such defects is just above the cholesterol rings and this should correspond to a hydrophobic local environment. It can be reached by the nitroxide of 10PC, but not 7PC. This would explain the jump in the fraction of non-polar component between 7 and 10PC, while further decrease in this fraction could be attributed to U-shaped conformations for higher values of *n*. These conformations put the nitroxide moiety back to the surface region with high water content, while the hydrocarbon chain mostly remains located in the hydrophobic part of the membrane.

Indeed, if we assume that the spin-labeled *sn*-chain takes on mostly the fully extended conformation, we would observe a similar jump after the nitroxide moiety reaches the hydrophobic core of the membrane, but with further increase in the *n* number the hydrogen-bonded fraction would decrease and quickly disappear.

Another limiting case suggests that the acyl-chain hydrocarbon tether connecting the nitroxide to the lipid head group can take all possible coil conformations of the chain. It will

put the possible position of the nitroxide of an *n*-PC spin label anywhere within a half sphere with a radius of the all-stretched conformation for the nitroxide tethers. This half sphere would rest on the membrane surface (cf. Fig.5). The ratio of hydrogen bonded/unbonded components would be opposite to the volume ratio of the spherical cap, which is cut off by the border of the hydrophobic core of the membrane, and the rest of the half sphere. If the cap height is half of the sphere radius, the ratio will be 2.2, similar to what we see for 7PC (Table 4). This observation can be then used to set (in a rather arbitrary fashion) the cutoff of the hydrophobic core at "3.5" PC, half of the acyl tether for 7PC in the fully extended conformation. The predictions of the components ratio obtained with this cutoff value by further applying the formula for the spherical cap are given in Table 5.
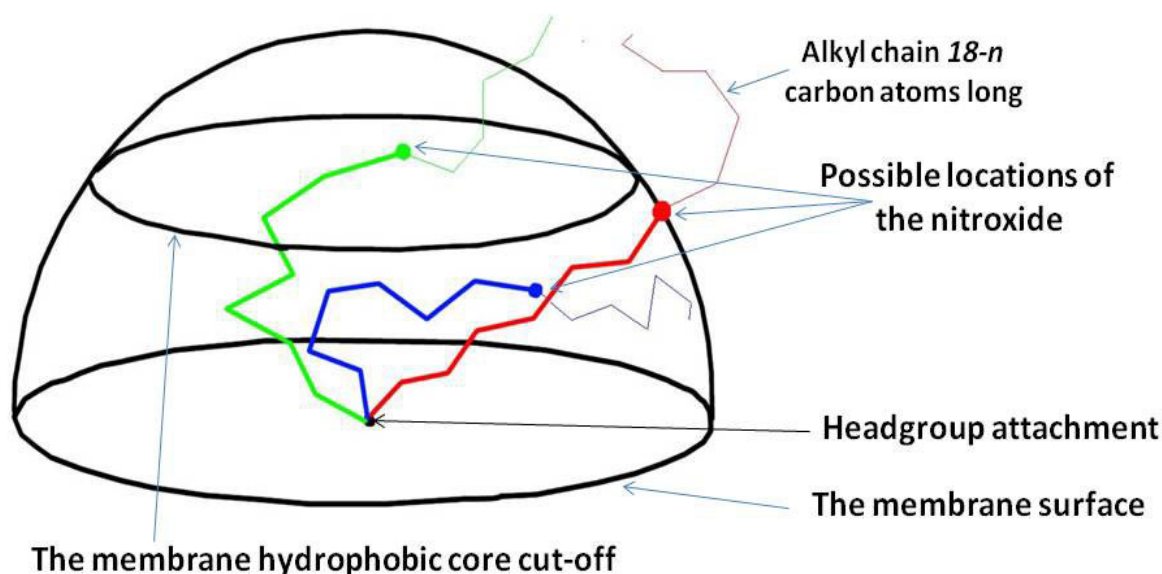

Figure 5. A model of random distribution of conformations of the spin label tethers for 7PC. It puts the spin label in some random position within the half-sphere. The spherical cap is the intersection of the area available for the nitroxide and the hydrophobic core of the membrane.

n-PC	5	7	10	12	14	16
HB/non-HB	7.2	2.2	1.01	0.74	0.58	0.48

Table 5. Estimates for the ratio of hydrogen bonded and non-hydrogen bonded components based on the simple model shown in Fig. 12. The location of the nitroxide moiety is considered in the hydrophobic core of the membrane if the distance to the membrane surface is more than half of the acyl tether for 7PC in the fully extended conformation ("3.5 PC").

Although this model is qualitatively better when compared to Table 4, it does not reproduce the observed abrupt drop between positions 7 and 10. Also, no model assuming some random distribution of nitroxide depth position would reproduce the decrease in the hydrophobic fraction with further increase in *n* beyond 10.

To better explain the observed effects one could assume some set of preferential depth positions in the membrane to be occupied by the nitroxide ring. These positions may be

areas of defects in the membrane structure, which can more easily accommodate a structure-disturbing nitroxide moiety than areas with compact alignment of hydrocarbon chains. One of the areas of such defects could start above the end of the rigid fused-ring system of cholesterol[37], which is about the level reachable by *n*-PC labels starting from *n*=9. Once the tether length is sufficient, nitroxides start populating these favorable locations causing the change in the component ratio. However, the preference of the nitroxide ring for the location in the hydrophobic part of a DMPC/Cholesterol or DPPC/Cholesterol membrane apparently does not completely overwhelm its affinity to some sites close to the membrane surface. It gives a partition-like distribution between the two sites which is observable in the spectrum of all *n*-PC labels with *n*>7 as two components.

A gradual increase in the hydrogen-bonded fraction between PC10 and PC16 can be also explained using this partition model. For an *n-PC* spin label, the same carbon atom of the nitroxide ring that is connected to the acyl tether also has a hydrocarbon tail with a length of *18-n* carbons attached. Bringing the nitroxide label of 10PC to the membrane surface will require, on the average, placing more hydrophobic CH_2 groups to the polar area than for 16PC. This will be associated with some energy penalty preventing the nitroxide of 10PC from leaving the hydrophobic core and affecting the partition. Note also a slight drop in the accessibility of the 10PC position for Ni^{2+} ions for cholesterol-free DMPC membranes, which may have the same origin.

3.2.2. DMPC and DPPC without cholesterol. Nitroxide moiety as a foreign body in the bilayer

It has been previously observed that in the absence of cholesterol, PC spin labels in DPPC[26] and DMPC[27] at rigid limit conditions have a strong broad background signal. This signal points at aggregation of spin labels and is most pronounced for the 7-12 PC positions. Since no significant signs of such aggregation are seen in the fluid phase of the membrane or in the gel phase in the presence of cholesterol, this aggregation can be specifically attributed to the gel or crystalline (sub-gel) state of pure-lipid membranes. Also, since diffusion in the gel phase is slow, one can expect hysteresis effects and effects of the sample-treatment procedure, see[38, 39].

Fig. 6 shows 240 GHz ESR spectra of PC spin labels in DMPC membranes without cholesterol. These spectra were recorded after the sample was slowly cooled from 295 to 85K within ~ 2 hours. As in the presence of cholesterol, two components with different g_{xx} are clearly discernible. However, another broad unresolved component, which is present for all spin labels but most pronounced for 7-12PC, follows a previously observed[26] pattern for DPPC at 250GHz . Our 240 GHz data for DPPC obtained under the same conditions as those for DMPC are very similar to the 250 GHz results by Earle et al.[26] and shown in Fig.7. A non-polar (non -hydrogen bonded) component similar to the non-polar component in membranes containing cholesterol can be identified by its characteristic g_{xx} value. However, there is an important and obvious difference between DMPC and DPPC at first inspection. In DPPC there is only one resolved component which shows the g_{xx} value corresponding to the non-hydrogen bonded state of the nitroxide, while in DMPC two components are clearly
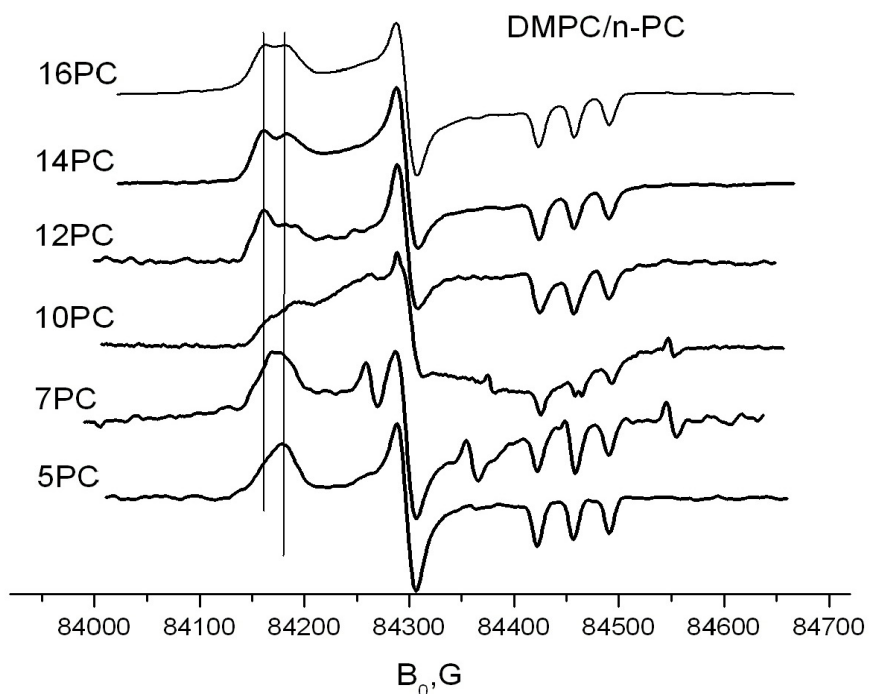
Figure 6. *n*-PC spin labels in DMPC with no cholesterol at 80-82K. The samples are gradually frozen in the flow of gaseous nitrogen. The vertical lines indicate g values of 2.00882 and 2.009435. (The additional superposition signal for 7PC originates from an occasional manganese impurity in the sample holder) (from [16]).
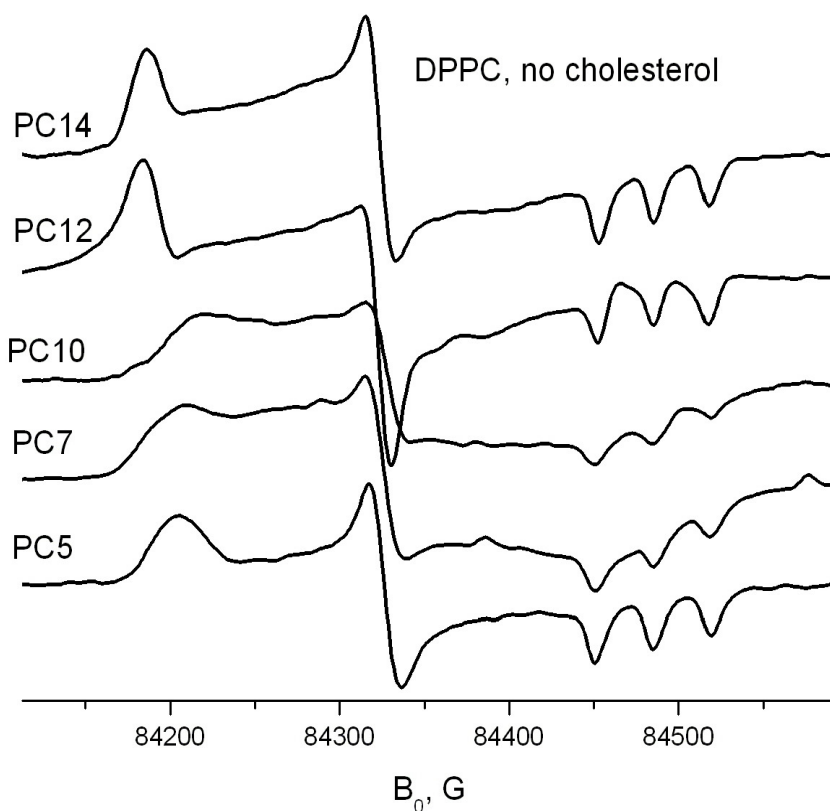

Figure 7. n-PC spin labels in DPPC with no cholesterol at 80-82K. The samples are gradually frozen in the flow of gaseous nitrogen (from [16]).

discernible in the spectrum. This observation is in good accord with the X-band results, which indicate a less polar environment reported by high values of n in DPPC compared to DMPC (cf. Table 3, Figs. 2A, 2C).

It is very unlikely that small structural differences between the gel phase bilayers of DMPC and DPPC[40, 41] cause dramatically different water penetration into these membranes and explain the presence of the hydrogen-bonded component in DMPC, but not DPPC. Moreover, it has been recently shown that water penetration into the membrane depends rather on the surface area of the lipid (which is nearly identical for DMPC and DPPC) than on the membrane thickness[42]. Thus, it makes the explanation of the difference between DMPC and DPPC through dramatically different water penetration very unlikely. Even more intriguing, the average environment of the nitroxide in DPPC looks, at the first glance, less polar in the absence of cholesterol, since no component with a clear peak at smaller g_{xx} can be detected, cf. Fig 8.
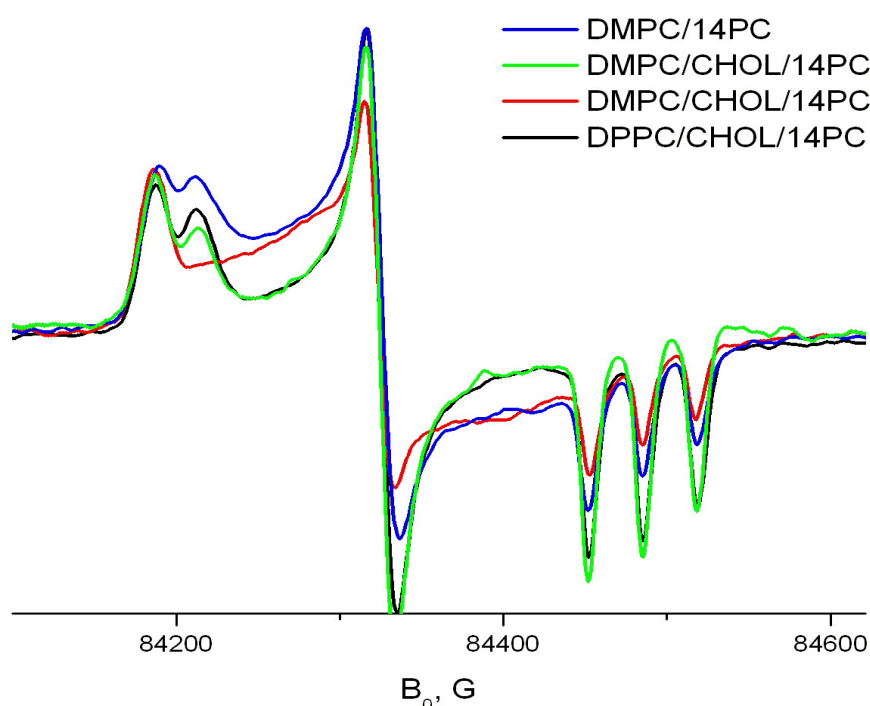

Figure 8. Comparison of 14 PC spin label in DMPC and DPPC with/without cholesterol. All samples are slowly frozen in the flow of gaseous nitrogen. While in the presence of cholesterol the spectra can be described as a superposition of two rigid-limit components, the most salient feature in the absence of cholesterol is a broad singlet-like background signal (from [16]).

However, the most salient feature of all spectra, both DMPC and DPPC, in the absence of cholesterol, is a broad singlet-like background signal which accounts for most of the spins. The location of spins responsible for this background is unclear. In Fig. 8 one can see an apparent broadening of the hydrogen-bonded component in DMPC and complete absence of this component in DPPC, concomitant with an increase in the background. A likely explanation for these observations is that the hydrogen-bonded and non hydrogen- bonded forms of PC spin labels aggregate differently. If the hydrogen bonded form is more prone to

aggregation than the non- bonded one, it likely becomes broader due to more interactions between spins. In the superposition, spectral peaks from this broad component are less intense and eventually, with an increase in broadening, not discernible at all. To test this hypothesis we cooled our samples very rapidly in an attempt to trap the hydrogen-bonded component before aggregation could occur.

Slow cooling vs. quick submerging into liquid nitrogen

Quantitative study of aggregation in the gel or subgel phases is difficult because of the slow diffusion rates and various hysteresis effects. For example, even though the gel phase of DPPC does not favor formation of gramicidin channels, it takes between an hour and several days for these channels to dissociate[39]. There are also indications pointing to a relatively slow time scale for aggregation of PC spin labels in the gel-phase. Fig. 9 shows saturation curves for 0.5 mol. % of 7PC in DMPC. At 19^{0}C, in the P$_\beta$ phase, this system show good saturation, with a P parameter of ~ 19. Saturation measurements performed immediately after cooling to 2^{0}C give a similarly high P value. However, after longer exposure at this temperature the P value starts to decrease and after several hours drops below 2. This increase in relaxation is very likely due to aggregation, and this aggregation appears to be a relatively slow process at 2^{0}C. Also, this increase in relaxation is reversible; return to 19^{0}C reverses the aggregation and the P value. Although a temperature of 2^{0}C should correspond to the subgel phase, the exact phase state of the lipid at this condition is not obvious due to likely supercooling, see below. It usually takes days at this temperature to form the L$_C$ phase, which then can be characterized by X-Ray diffraction.
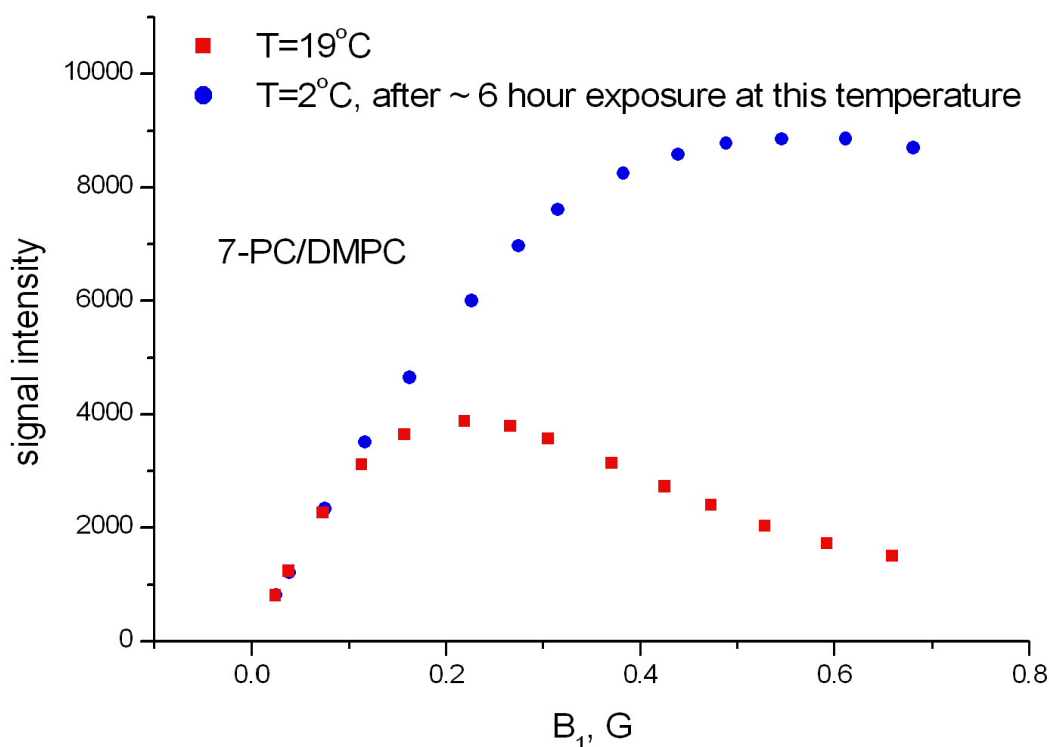

Figure 9. Change in relaxation curve of 7PC in DMPC under exposure at 2^{0}C. This increase in relaxation occurs gradually within several hours and it can be completely reversed by a brief exposure at 19^{0}C (from [16]).

Previously, similar observations of exclusion of 5PC spin labels from DPPC after exposure at 0^0C by using Saturation Transfer ESR[43] were attributed to formation of a sub-gel phase.

We expected that quick freezing (within ~ 0.2s) of the sample by instantly submerging into liquid nitrogen should substantially eliminate these slow lipid rearrangement effects compared to the standard slow cooling procedure using a flow cryostat. Indeed, spectra recorded after this simple quick-freeze procedure were different from the spectra obtained by gradual cooling in a flow of gaseous nitrogen. As seen in Fig. 10A the spectrum of 14PC in DPPC does not have a broad singlet-like component and can be well simulated by a simple superposition of two rigid limit spectra with g_{xx} of 2.00943 and g_{xx}= 2.00882.
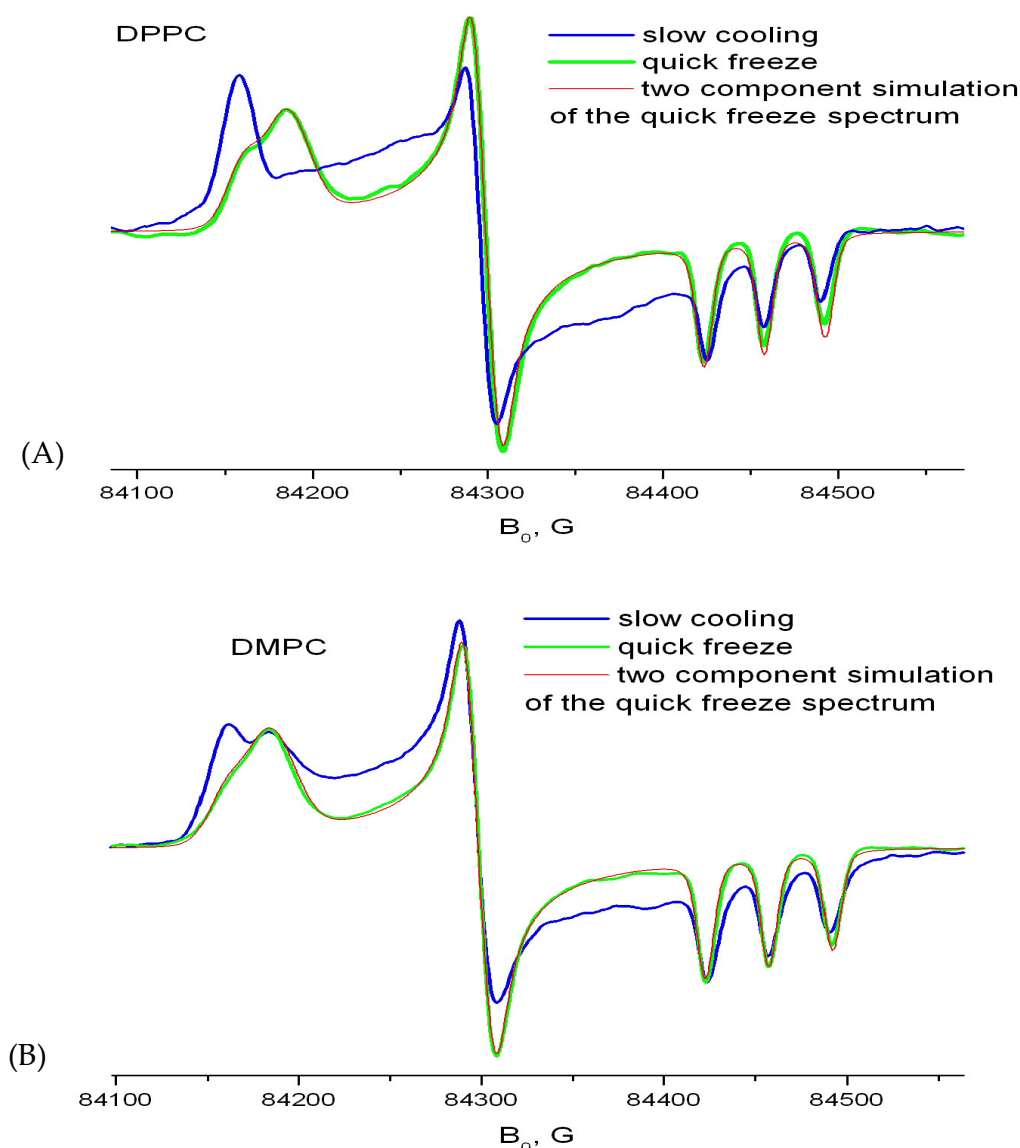

Figure 10. 14PC in DPPC (A) and DMPC (B): gradual cooling vs. quick freeze by submerging into liquid nitrogen. The spectra are recorded at 80-82K. In the case of quick freezing the broad unresolved component disappears and the spectrum can be well described as a superposition of HB/non-HB forms of the nitroxide. The HB/non-HB ratio is 2.2:1 for DPPC and 3.1:1 for DMPC (from [16]).

Importantly, most 14PC spins are present in the form of the hydrogen bonded component, which has a fraction greater than the non-bonded one by a 2.2:1 ratio.

As seen from Fig 11, quick freezing helps to dramatically decrease the amount of the broad background signal and yields well resolved rigid-limit spectra even when a standard cooling procedure results in nearly unresolvable, broad-feature spectra.
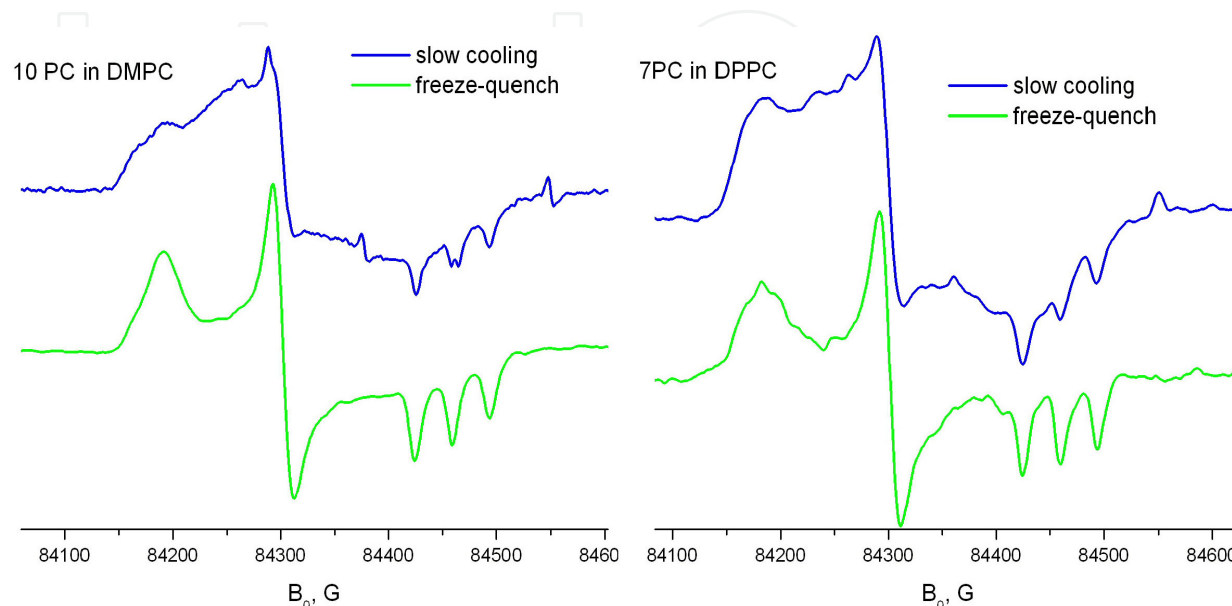

Figure 11. Obtaining better resolved spectra by quick freezing in liquid nitrogen (from [16]).

Nitroxides in the L'$_\beta$ phase – an analogy to bulk crystallizing solids

One of the possible artifacts of using molecular probes as reporters in biological and model membranes is their exclusion from the membrane interior to the membrane surface. Such exclusion of certain molecules or structural units is a natural feature of membrane biological function. For example, exclusion of tryptophans and their affinity to the membrane interface is an important factor in lipid-protein interactions and stabilization of certain conformations of transmembrane protein/peptides[44]. Exclusion from the bilayer and formation of some U-shaped conformations have been known for a long time for a number of fluorescent labels[7, 9, 11].

Spin labels are usually considered as more adequate molecular probes for lipid bilayers, as evidenced by studies in fluid membranes (see Introduction). However, our current study shows that in the gel phase the situation is different. Several ESR parameters (accessibility for Ni^{2+} ions absorbed on the membrane surface, hyperfine tensor and g-tensor components) unambiguously indicate that in the gel phase a substantial fraction of nitroxide is located in the membrane region with high water content. Pure lipids DMPC and DPPC form the L'$_\beta$ "tilted gel" phase with densely packed and relatively well ordered hydrocarbon chains. The ability of nitroxide groups on spin labeled stearic acids to be excluded from hydrocarbon environments and form U-shaped conformations has been previously reported[12, 13]. In principle, formation of the L'$_\beta$ phase can be compared with freezing of a bulk three-dimensional solvent. In this case solutes are excluded from crystallizing solvent and form some regions with high local concentration. If the solute is a nitroxide radical, freezing of its

solution in non glass-forming media is well known to yield a broad signal similar to one observed in DMPC or DPPC without cholesterol (Figs 6, 7).

In the case of a lipid in the gel phase the complete exclusion of spin labels into a separate phase with a high spin concentration appears to take two steps. The first one, exclusion of nitroxides from the hydrophobic area of the membrane, occurs once the lipid forms an L_{β}' or even a P_{β} phase (cf. Fig 3 for 19^{0}C, the P_{β} phase of DMPC, also the quick-freeze spectra in Fig. 10). The second stage, which is a formation of separate phase by these bent-conformation molecules, can be attributed to lateral aggregation in the supercooled gel, possibly at the gel/subgel phase transition.

Although formation of subgel phases was initially observed after storing a multilamellar suspension of DPPC at ~0^{0}C for several days[45], there are reports of quicker gel/subgel transformations in DPPC and DMPC. For example, in one protocol[46] the subgel (SGII) phase in DPPC forms at about 7^{0}C upon cooling at 2^{0}C/min. These conditions are very similar to cooling conditions observed in our "slow cooling" experiment – and, in general, the cooling conditions usually existing in standard helium/nitrogen cryostats. For DMPC, formation of the subgel phase was reported after incubation at temperatures of -5^{0}C or lower for 2h[47]. But, the kinetics of subgel formation is complex[48] and in some cases the final subgel phase contains spectroscopic features characteristic for the L_{β}' phase[49]. It could be possible that aggregation of spin labels does not require a complete transformation into the subgel phase, in the sense of giving a clean X-ray pattern, and can happen sooner during cooling.

Again, we would like to stress that exclusion of nitroxides from the hydrophobic membrane core occurs in all gel phases and is a separate effect from the succeeding lateral aggregation in the supercooled gel phase.

Our quick freeze vs. slow cooling experiments can also help answer an important question about the nature of the two components in the 240GHz spectrum. Does the component with a larger g_{xx} correspond to the location of the nitroxide in the hydrophobic part of the membrane? Or both components arise from equilibrium of the hydrogen-bonded/non-hydrogen bonded forms in the same location, like TEMPONE in ethanol (cf. Fig. 1A)? The different aggregation behavior of spins contributing into these components points to their different location. That is, the major hydrogen-bonded component comes from nitroxides excluded from the hydrophobic part into the area with high water content, while the minor non-polar component may arise from spins somehow trapped in the defects of the hydrophobic membrane core.

3.3. What about biological membranes?

The gel phase rarely exists in biological membranes and the subgel phase is unknown for them. However, polarity measurements in frozen natural membranes using PC spin labels can also be affected by the affinity of spin labels to some structural defects, especially in the presence of proteins. For example, all PC labels in mixtures of DPPC with gramicidin A show about the same g_{xx} value, indicative of the same polarity[26], most likely due to an

interaction with the peptide's α-helical structure. Also, natural membranes usually have complex lipid head group composition and variety of lengths and unsaturation in acyl chains. This can affect the free volume available for spin labels both in the hydrophobic core and in the membrane interface. Fig. 12 shows 240 GHz spectra for 14PC in egg-yolk lecithin with and without cholesterol.
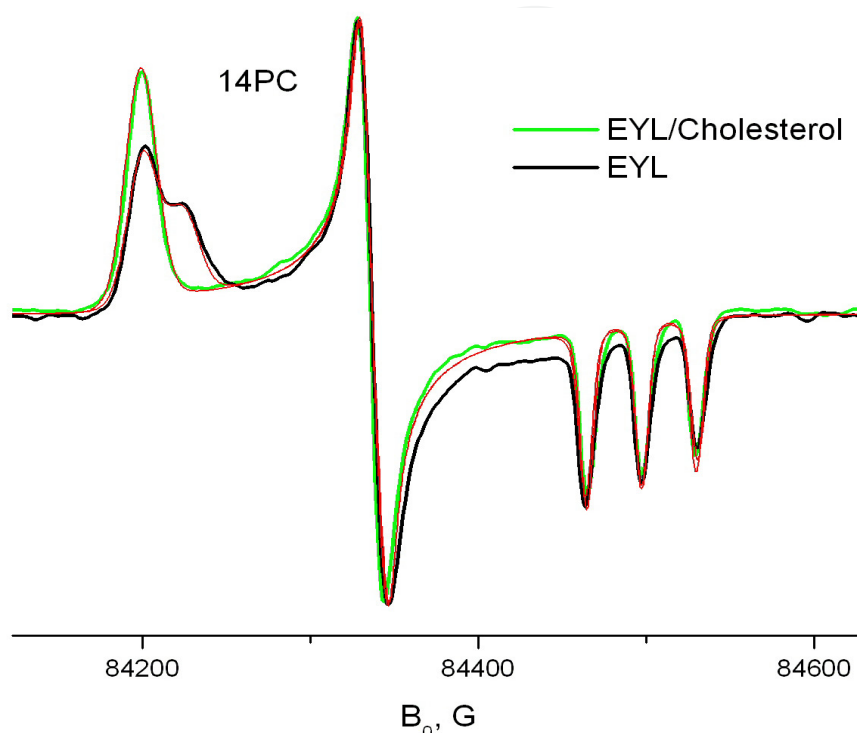

Figure 12. 14 PC in EYL with and without cholesterol at 82K. The samples are gradually frozen in the flow of gaseous nitrogen. The corresponding one and two-component (the ratio of components with $g_{xx}=2.009410$ and 2.008820 is 0.5) rigid limit simulations are shown in red (from [16]).

One can see that, similar to DMPC and DPPC membranes, the fraction of the hydrogen-bonded component drops with addition of cholesterol (cf. Figs 4 and the quick-freeze spectra in Fig.10). However, compared to DMPC and DPPC membranes this fraction in EYL is lower. Actually, in EYL/Cholesterol only a non-polar component can be observed in the spectrum. It can be explained by the presence of a double bond in the acyl chain of EYL. This unsaturated bond has a kink, which disrupts the packing of lipids. It creates extra free space in the hydrophobic core of the membrane[50], and thus may shift the partition of nitroxides in favor of the membrane interior. Also, a variety of headgroups may improve packing in the polar head area, additionally forcing nitroxides into the hydrophobic core.

3.4. Summary

The ESR parameters of PC spin labels in frozen membranes do not simply represent the membrane polarity or water penetration profile. Instead, they show a distribution between hydrogen-bonded (HB) and non-hydrogen bonded (non-HB) states, which is affected by a number of factors in the membrane composition. In frozen lipid membranes at 240 GHz *n-*

PC labels with $n > 7$ usually show two-component ESR spectra corresponding to HB and non-HB states of the nitroxide. In DMPC and DPPC membranes without cholesterol the ESR spectra recorded after gradual sample cooling show a broad background signal as well. But if the sample is instantly frozen, the broad background signal is absent and one observes mainly the HB component. We attribute the HB component for $n \geq 10$ to bent conformations of the nitroxide tethers. Such conformations at 9 GHz ESR manifest themselves in apparent "polar" A_{zz} values and increased accessibility of the nitroxide to aqueous Ni^{2+} ions. These bent conformations prevail in the absence of cholesterol due to the tendency of the pure gel phase to exclude nitroxides, similar to the exclusion of solutes from crystallizing solvents. The formation of a separate phase of spin-labeled lipid (i.e. precipitate) manifests itself in the broad background ESR signal and occurs slowly in the supercooled gel. In membranes with cholesterol the observed HB/ non-HB ratio can best be described by a partition-like equilibrium between nitroxides located in defects of lipid structure in the hydrophobic core of the membrane and those close to the membrane surface.

Abbreviations

HF ESR, HFHF ESR: High Field ESR, High Field/High Frequency ESR

DMPC: 1,2-dimyristoyl-*sn*-glycero-3-phosphocholine

DPPC: 1,2-dipalmitoyl-*sn*-glycero-3-phosphocholine

EYL: egg yolk lecithin

n-PC spin labels: 1-palmitoyl-2-stearoyl-(n-doxyl)-sn-glycero-3-phosphocholines

TFE: 2,2,2-trifluoroethanol

MCH: methylcyclohexane

TEMPO: 2,2,6,6-tetramethylpiperidine-N-oxyl

TEMPOL, 4-Hydroxy-TEMPO: 4-hydroxy-2,2,6,6-tetramethylpiperidine-N-oxyl

TEMPONE, Oxo-TEMPO: 4-oxy-2,2,6,6-tetramethylpiperidine-N-oxyl

Author details

Boris Dzikovski and Jack Freed
National Biomedical Center for Advanced ESR Technology (ACERT),
Department of Chemistry and Chemical Biology, Baker Laboratory,
Cornell University, Ithaca, NY, USA

Acknowledgement

4. References

[1] Swamy, M.J., L. Ciani, M. Ge, A.K. Smith, D. Holowka, B. Baird, and J.H. Freed, *Coexisting Domains in the Plasma Membranes of Live Cells Characterized by Spin-Label ESR Spectroscopy.* Biophys. J., 2006. 90: p. 4452-4465.

[2] Altenbach, C., D.A. Greenhalgh, H.G. Khorana, and W.L. Hubbell, *A collision gradient method to determine the immersion depth of nitroxides in lipid bilayers: application to spin-labeled mutants of bacteriorhodopsin.* Proc. Natl. Acad. Sci. USA., 1994. 91: p. 1667-1671.

[3] Marsh, D., *Polarity and permeation profiles in lipid membranes.* Proc. Natl. Acad. Sci. USA 2001. 98: p. 7777-7782. .

[4] Dzikovski, B., V.A. Livshits, and D. Marsh, *Oxygen permeation profile in lipid membranes: nonlinear spin-label EPR. .* Biophys. J. , 2003. 85: p. 1005-1012.

[5] Marsh, D., A. Watts, R.D. Pates, R. Uhl, P.F. Knowles, and M. Esmann, *ESR spin-label studies of lipid-protein interactions in membranes.* Biophys. J., 1982. 37: p. 265-274.

[6] Costa-Filho, A.J., P.P. Borbat, R.H. Crepeau, M. Ge, and J.H. Freed, *Lipid-Gramicidin Interactions: Dynamic Structure of the Boundary Lipid by 2D-ELDOR.* Biophys. J., 2003. 84: p. 3364-3378.

[7] Ashcroft, R.G., K.R. Thulborn, J.R. Smith, H.G.L. Coster, and W.H. Sawer, *Perturbation to lipid bilayers by spectroscopic probes as determined by dielectric measurements.* BBA, 1980. 602: p. 299-308.

[8] Krishnan, K.S. and P. Balaram, *Perturbation of lipid structures by fluorescent probes.* FEBS Lett., 1975. 60: p. 419-422.

[9] Chattopadhyay, A. and E. London, *Parallax Method for Direct Measurement of Membrane Penetration Depth Utilizing Fluorescence Quenching by Spin-Labeled Phospholipidst.* Biochemistry, 1987. 26: p. 39-45.

[10] Vogel, A., H.A. Scheidt, and D. Huster, *The distribution of lipid attached spin probes application to membrane protein topology.* Biophysical Journal, 2003. 85: p. 1691-1701.

[11] Cadenhead, D.A., B.M.J. Keller, and F. Muller-Landau, *A comparison of a spin-label and a fluorescent cell membrane probe using pure and mixed monomolecular films.* Biochim. Biophys. Acta., 1975. 382: p. 253-259.

[12] Dzikovski, B. and V. Livshits, *EPR spin probe study of molecular ordering and dynamics in monolayers at oil/water interfaces.* PCCP, 2003. 5: p. 5271-5278

[13] Baglioni, P., L. Dei, E. Rivara-Minten, and L. Kevan, *Mixed Micelles of SDS/$C_{12}E_6$ and DTAC/$C_{12}E_6$, Surfactants.* J. Am. Chem. Soc., 1993. 115: p. 4286-4290.

[14] Marsh, D., *Spin-Label EPR for Determining Polarity and Proticity in Biomolecular Assemblies: Transmembrane Profiles.* Appl. Magn. Reson., 2010. 37: p. 435-454.

[15] Ellena, J.F., S.J. Archer, R.N. Dominey, B.D. Hill, and D.S. Cafiso, *Localizing the nitroxide group of fatty acid and voltage-sensitive spin-labels in phospholipid bilayers.* BBA, 1988. 940: p. 63-70.

[16] Dzikovski, B., D. Tipikin, and J.H. Freed, *Conformational Distributions and Hydrogen Bonding in Gel and Frozen Lipid Bilayers: A High Frequency Spin-Label ESR Study.* J. Phys. Chem. B., 2012. in press: p. DOI: 10.1021/jp211879s.

[17] Kawamura, T., S. Matsunami, and T. Yonezawa, *Solvent effects on the g-value of di-t-butyl nitric oxide.* Bull. Chem. Soc. Japan, 1967. 40: p. 1111-1115.

[18] Smirnov, A.I. and T.I. Smirnova, *Resolving domains of Interdigitated Phospholipid Membranes with 95 GHz Spin labeling EPR.* Appl. Magn. Reson., 2001. 21: p. 453-467.

[19] Smirnova, T.I., A.I. Smirnov, S.V. Pachtchenko, and O.G. Poluektov, *Geometry of Hydrogen Bonds Formed by Lipid Bilayer Nitroxide Probes: A High Frequency Pulsed ENDOR/EPR Study.* JACS, 2007. 129: p. 3476-3477.

[20] Bordignon, E., H. Brutlach, L. Urban, K. Hideg, A. Savitsky, A. Schnegg, P. Gast, M. Engelhard, E.J.J. Groenen, K. Möbius, and H.-J. Steinhoff, *Heterogeneity in the Nitroxide Micro-Environment: Polarity and Proticity Effects in Spin-Labeled Proteins Studied by Multi-Frequency EPR.* Appl. Magn. Reson., 2010. 37: p. 391-403.

[21] Hwang, J.S., R.P. Mason, L.-P. Hwang, and J.H. Freed, *Electron Spin Resonance studies of Anisotropic Rotational Reorientation and Slow Tumbling in Liquid and Frozen Media. III. Perdeuterated 2,2,6,6-Tetramethyl-4-piperidone-N-Oxide and An Analysis of Fuctuating Torques.* J. Phys. Chem., 1975. 79: p. 489-511.

[22] Pavone, M., A. Sillanpää, P. Cimino, O.Crescenzi, and V. Barone, *Evidence of Variable H-Bond Network for Nitroxide Radicals in Protic Solvents.* J. Phys. Chem. B, 2006. 110: p. 6189-16192.

[23] Erilov, D.A., R. Bartucci, R. Guzzi, A.A. Shubin, A.G. Maryasov, D. Marsh, S.A. Dzuba, and L. Sportelli, *Water concentration Profiles in Membranes Measured by ESEEM of Spin-Labeled Lipids.* J. Chem. Phys. B, 2005. 109: p. 12003-12013.

[24] Owenius, R., M. Engström, M. Lindgren, and M. Huber, *Influence of solvent polarity and hydrogen bonding on the EPR parameters of a nitroxide spin label studied by 9-GHz and 95-GHz EPR spectroscopy and DFT calculations.* J. Phys. Chem. A, 2001. 105: p. 10967-10977.

[25] Plato, M., H.-J. Steinhoff, C. Wegener, J.T. Törring, A. Savitsky, and K. Möbius, *Molecular orbital study of polarity and hydrogen bonding effects on the g and hyperfine tensors of site directed NO spin labelled bacteriorhodopsin.* Molecular Physics, 2002. 100: p. 3711-3721.

[26] Earle, K.A., J.K. Moscicki, M. Ge, D.E. Budil, and J.H. Freed, *250-GHz Electron Spin Resonance Studies of Polarity Gradients Along the Aliphatic Chains in Phospholipid Membranes.* Biophys. J., 1994. 66: p. 1213-1221.

[27] Kurad, D., G. Jeschke, and D. Marsh, *Lipid Membrane Polarity Profiles by High-Field EPR.* Biophysical Journal, 2003. 85: p. 1025-1033.

[28] Marsh, D., D. Kurad, and V.A. Livshits, *High-field spin-label EPR of lipid membranes* Magn. Reson. Chem., 2005. 43: p. S20-S25.

[29] Budil, D.E., K. Earle, and J.H. Freed, *Full determination of the rotational diffusion tensor by electron paramagnetic resonance at 250GHz. .* J. Phys. Chem., 1993. 97: p. 1294-1303.

[30] Marsh, D., *Membrane water-penetration profiles from spin labels.* Eur. Biophys. J., 2002. 31: p. 559-562.

[31] Bartucci, R., D.A. Erilov, R. Guzzi, L. Sportelli, S.A. Dzuba, and D. Marsh, *Time-resolved electron spin resonance studies of spin-labeled lipids in membranes.* Chemistry and Physics of Lipids, 2006. 141: p. 142-157.

[32] Berendsen, H.J.C. and S.J. Marrink, *Molecular dynamics of water transport through membranes: Water from solvent to solute.* Pure&Appl.Chem., 1993. 65: p. 2513-2520.

[33] Lande, M.B., J.M. Donovan, and M.L. Zeidel, *The relationship between membrane fluidity and permeabilities to water, solutes, ammonia, and protons.* J. Gen. Physiol., 1995. 106: p. 67-84.

[34] Carruthers, A. and D.L. Melchior, *Studies of the relationship between bilayer water permeability and bilayer physical state.* Biochemistry, 1983. 22: p. 5797-5807.

[35] Rubenstein, J.L., B.A. Smith, and H.M. McConnell, *Lateral diffusion in binary mixtures of cholesterol and phosphatidylcholines.* Proc. Natl. Acad. Sci. U.S.A., 1979. 76: p. 15-18.

[36] Lee, A.G., *Analysis of the Defect Structure of Gel-Phase Lipid.* Biochemistry 1977. 16: p. 835-841.

[37] Yeagle, P.L., *The role of cholesterol in the biology of cells*, in *The structure of biological membranes.* , P.L. Yeagle, Editor. 2005, CRC press: Boca Raton - London - New York - Washington DC. p. 243-254.

[38] Dzikovski, B.G., P.P. Borbat, and J.H. Freed, *Spin-labeled gramicidin A: Channel formation and dissociation.* Biophysical Journal, 2004. 87(5): p. 3504-3517.

[39] Dzikovski, B.G., K.A. Earle, S.V. Pachtchenko, and J.H. Freed, *High-field ESR on aligned membranes. A simple method to record spectra from different membrane orientations in the magnetic field.* Journal of magnetic resonance, 2006. 179: p. 273-277.

[40] Tristram-Nagle, S., Y. Liu, J. Legleiter, and J.F. Nagle, *Structure of gel phase DMPC determined by x-ray diffraction.* Biophysical Journal, 2002. 83(6): p. 3324-3335.

[41] Nagle, J.F. and S. Tristram-Nagle, *Structure of lipid bilayers.* Biochimica et Biophysica Acta, Reviews on Biomembranes, 2000. 1469(3): p. 159-195.

[42] Mathai, J.C., S. Tristram-Nagle, J.F. Nagle, and M.L. Zeidel, *Structural Determinants of Water Permeability through the Lipid Membrane.* J. Gen. Physiol., 2007. 131: p. 69-76.

[43] Páli, T., R. Bartucci, L. Horváth, and D. Marsh, *Kinetics and dynamics of annealing during sub-gel phase formation in phospholipid bilayers. A saturation transfer electron spin resonance study.* Biophys. J., 1993. 64: p. 1781-1788.

[44] Sun, H., D.V. Greathouse, O.S. Andersen, and R.E.I. Koeppe, *The preference of tryptophan for membrane interfaces.* J. Biol. Chem., 2008. 283: p. 22233-22243.

[45] Chen, S.C., J.M. Sturtevant, and B.J. Gaffney, *Scanning calorimetric evidence for a third phase transition in phosphatidylcholine bilayers* Proc. Natl. Acad. Sci. U.S.A., 1980. 77: p. 5060-5063.

[46] Koynova, R., B.G. Tenchov, S. Todinova, and P.J. Quinn, *Rapid Reversible Formation of a Metastable Subgel Phase in Saturated Diacylphosphoatydylcholines.* Biophys. J., 1995. 68: p. 2370-2375.

[47] Chang, H.H., R.K. Bhagat, R. Tran, and P. Dea, *Subgel Studies of Dimyristoyphosphatidylcholine Bilayers.* J. Phys. Chem. B, 2006. 110: p. 22192-22196.

[48] Tristram-Nagle, S., R.M. Suter, W.-J. Sun, and J.F. Nagle, *Kinetic of subgel formation in DPPC: X-ray difraction proves nucleation-growth hypothesis.* BBA, 1994. 1191: p. 14-20.

[49] Lewis, R.N.A.H. and R.N. McElhaney, *Structures of the subgel phases of n-saturated diacyl phosphatidylcholine bilayers:FTIR spectroscopic studies of $^{13}C=O$ and ^2H labeled lipids.* Biophys. J., 1992. 61: p. 63-77.

[50] Rawicz, W., K.C. Olbrich, T.J. McIntosh, D. Needham, and E. Evans, *Effect of chain length and unsaturation on elasticity of lipid bilayers.* Biophys. J., 2000. 79: p. 328-339.

[51] *CRC Handbook of Chemistry and Physics, 91st Edition*, ed. W.M. Haynes. 2010, Boulder, CO National Institute of Standards and Technology.

[52] Dzikovski, B., D.S. Tipikin, V. Livshits, K.A. Earle, and J.H. Freed, *Multi-frequency ESR Study of Spin-Labeled Molecules in Inclusion Compounds with Cyclodexrins.* PCCP, 2009. 11: p. 6676-6688.